Ferroelectric Properties Study of Si 0.5 Sn 0.5 ZnO 3 Thin Films Deposited by PLD Technique

Ahmed I. Ali (ahmed_Ali_2010@techedu.helwan.edu.eg)
Helwan University
A. B. El Basaty
Helwan University
W. Abbas
Arab Academy for Science Technology and Maritime Transport
M. M. Ahmed
Helwan University

Research Article

Keywords: Polarization, Ferroelectric thin film, Si0.5Sn0.5ZnO3, current density, buffer layer, STO, substrate

Posted Date: August 18th, 2022

DOI: https://doi.org/10.21203/rs.3.rs-1946566/v1

Abstract

$Si_{0.5}Sn_{0.5}ZnO_3$ thin films deposited on two different substrates (STO) and (MgO) using pulsed laser deposition technique. The current study aims to explore both effects of Si-doped in $SnZnO_3$ and the rule of the $SrTiO_3$ (STO) buffer layer in the adjustment of the ferroelectricity of the grown samples. Structure, morphology, uniformity, thickness, and the crack-free film growth are confirmed using X-Ray diffraction, atomic force microscopy (AFM) and scanning electron microscopy (SEM). Both resistivity and carriers's mobility of $Si_{0.5}Sn_{0.5}ZnO_3$ film's values are 3.22×10^3, 7.35×10^7 $\Omega^{-1}.m^{-1}$ (semiconductor) and 4.31×10^3, 63.1 m/(V·s) (insulator) on MgO and STO substrates, respectively. The P-E loops show Lossy capacitor response and Non-linear ferroelectric response for MgO, and STO substrates, respectively. Furthermore, the ferroelectricity parameters of the $Si_{0.5}Sn_{0.5}ZnO_3$ films deposited on the $SrTiO_3$ layer are improved orders of magnitude compared to the thin film on the MgO substrate to be suitable for Ferroelectric RAM applications.

I. Introduction

The importance of industrial nanotechnology application requires special properties in the smart material. The ferroelectric materials have a variety of attractive properties that exhibit a dependence on different factors including strain, electric field, temperature, …etc. Therefore, these materials valuable in a variety of applications involving sensors, energy storage memory cells, capacitors, actuators. However, establishing narrative composites has powerful and enduring polarization, ferroelectric class, could produce new properties to be useable in energy harvesters. When electric field is applied to these materials exhibited a permanent electric dipole moment and increased the polarization. Several devices required special properties in ferroelectric materials. The suitable ferroelectric materials for these devices are $BaTiO_3$ (BT) family that were extensive investigated with a remarkable benefit [6)2)3)4)5)9)]. $BaTiO_3$ is a lead-free ceramic and environmentally save. In our previous studies about $BaTiO_3$, there are many factors have been investigated like doping (Al, La), doping elements and sites (A-site and B-site), deposition methods, concentration levels, form of samples (ceramics or thin films),..etc.[1)1)3)4)5)6)7)8)9)10)11)12)13)]

$BaTiO_3$, has numerous advantages like an exceptionally a large rest polarization, lower coercive field, excellent mechanical intensity, and with doping the composition can produce applications in ferroelectric devices[14)]. Further, $BaTiO_3$ thin films have been used as optical waveguide in electrical and/or optical devices.[15)] Additionally, it is achievable to realize novel component to be usable in nano-photonic applications for nanodevice in the new generation of devices.[16)]

Perovskite $ZnSnO_3$ is an environmentally friendly exhibited piezoelectric/ferroelectric properties which can harvest energy devoid of electrical pushing.[17)] The morphology of $ZnSnO_3$ is nanocube with nano-size. The crystal structure is rhombohedral consists of two octahedral SnO_6 and ZnO_6. It reported that, every octahedron has both three long bonds and three short bonds, which results different positions for

Sn and Zn atoms from the center of octahedron, inducing the non-centrosymmetry and exhibited ferroelectricity.[17),18),19),20)]

In the literature reviews, the Silicon element can be used for doping in ceramics which is is an efficient method to adjust the ferroelectric properties.[21)22)] Doping $SnZnO_3$ with Si induce dielectric states like behavior. The $SrTiO_3$ layers have improved the films properties and crystalline phase orientation, The STO layer can decrease the mismatch between the films and the substrata. The paraelectric or ferroelectric phases changed with doping elements and level of doping ratio of Si in $SnZnO_3$ which produce both of unusually large capacitance values and the film can be stable with temperature.

Doping process can be in A-site to achieve higher dielectric constant. Moreover, the layer of $SrTiO_3$ on the substrate can prevent mismatch of the lattice parameters (between perovskite thin films $Si_{0.5}Sn_{0.5}ZnO_3$ and substrate MgO). Based on above view point, the improvement of the ferroelectricity state of $SnZnO_3$ ceramic thin films for Fe-RAM usage can be done by choosing a correct growing conditions[22)] and method,[15)22)30)31)32)] doping,[23)24)25)26)27)28)29)] and type of substrates.[12)] Therefore, our goal in this study is adjusting the factors included, doping level, doping element, method of deposition, substrates and deposition conditions. Here doping element has been chosen to be Si-element with doping level of 0.5, to replace Sn with Si ions, because Si element is low cost and save. In addition to select the growing method (PLD Method) as well as the substrate MgO and buffer layer ($SrTiO_3$).

In this study we explore both effects of Si-doped in $SnZnO_3$ and $SrTiO_3$ buffer layer on the ferroelectric properties of the $Si_{0.5}Sn_{0.5}ZnO_3$ thin films. Ceramic $Si_{0.5}Sn_{0.5}ZnO_3$ thin films were fabricated on MgO and $SrTiO_3$/MgO substrates. The structure and morphology of the $Si_{0.5}Sn_{0.5}ZnO_3$ were characterized by XRD, SEM, AFM. In addition, polarization-field dependence of $Si_{0.5}Sn_{0.5}ZnO_3$ thin films was investigated. Electric properties of the films were verified.

I I. Experiments

a)Targets preparations:

Both $SrTiO_3$ and $Si_{0.5}Sn_{0.5}ZnO_3$ ceramics targets were manufactured by a solid-state reaction method. Chemicals of $SrCO_3$ (4N), TiO_2 (4N), SiO_2 (3N), and SnO_2 (4N) powders with high purities were bought from Aldrech. The powders were deeply grinded using a gate mortar for 2h. The mixture was calcined in alumina crucible for 3h at 600^{o}C in muffle furnace. Again the powder was grinded. Further, the obtained powders were fired at 1100 ^{o}C for 5 hours in programmable muffle furnace. The powder was molded into a circular pellet (Thickness 3 ~ 4 mm and radius 1.5 cm width) under a uniaxial pressure of 10 MPa. This process was followed by cold-isostatically pressing under 150 MPa for 10 min. Finally, the two targets ($SrTiO_3$ and $Si_{0.5}Sn_{0.5}ZnO_3$) are ready for deposition after test the crystal structure using X-ray diffraction (XRD) (Rigagu RU 300).

b) Thin films preparations:

Firstly, the $SrTiO_3$ ceramic thin films deposited on $MgO/TiO_2/SiO_2/Si$ (MgO) substrates using a $SrTiO_3$ target by Pulsed laser deposition. The $SrTiO_3/MgO/TiO_2/SiO_2/Si$ ($SrTiO_3$) films is ready to be substrate for the deposition of $Si_{0.5}Sn_{0.5}ZnO_3$. Secondly, The $Si_{0.5}Sn_{0.5}ZnO_3$ thin films were grown on MgO and $SrTiO_3$ substrates using pulsed laser deposition. The deposition take place using a KrF laser (Lambda Physik LPX200) working at a wavelength of 248 nm, was employed to grow $Si_{0.5}Sn_{0.5}ZnO_3$ thin films on MgO and $SrTiO_3$ substrates. The films were produced using a repetition rate of 5 Hz, fluency of 2.5 J/cm^2, the space between the target and substrate was ~ 4 cm. The substrate temperature was 550°C with an oxygen partial pressure of 10 mTorr. Annealing at 650 °C for 120 min and 240 min take place for $Si_{0.5}Sn_{0.5}ZnO_3$ thin films on MgO and $SrTiO_3$ substrates, respectively. The films for naturally cooled to room temperature in high oxygen pressure of 750 mTorr to re-oxidize the grown films.

c) Thin films characterization

The crystal structure of the $Si_{0.5}Sn_{0.5}ZnO_3$ films investigated using X-ray diffraction. The lattice parameters were studied from XRD data ($\theta - 2\theta$ patterns using Rigagu RU 300) with CuK_α radiation of wavelength 0.15408 nm. Both surface morphology and thickness of the thin films were detected using field emission scanning electron microscope (FE-SEM, JEOL JSM-7500F), the thickness as measured by a cross-sectional view of FE-SEM be 150 and 220 nm for the $Si_{0.5}Sn_{0.5}ZnO_3$ films grown on MgO and $SrTiO_3$ substrates, respectively.

To manufacture the Pt top electrodes on $Si_{0.5}Sn_{0.5}ZnO_3$ films, RF magnetron sputtering was used. The electrodes thicknesses in the form of dots 100 μm and 100 nm over the $Si_{0.5}Sn_{0.5}ZnO_3$ thin films on the MgO and STO substrates. After growing the top electrodes, the films were annealed at 350°C for ten minutes preceding to acquiring ferroelectric hysteresis loops (P-E), which were measured using an RT66A (Radiant Technologies, Inc.) system. The current density was investigated using a Keithley 2636A semiconductor parameter analyzer. Electrical parameters of $Si_{0.5}Sn_{0.5}ZnO_3$ thin films on MgO and STO substrates were measured using Hall experiment.

I I I. Results And Discusion

The X-Ray diffraction:

Fig. 1 (a) presented the patten of the $Si_{0.5}Sn_{0.5}ZnO_3$ ceramic target prepared using the solid-state reaction method. The pattern of the target investigated in the range of 2θ (20^o ~75^o). The pattern has been indexed with $SnZnO_3$ except only 4 peaks at 2θ equals 27 ^{o}, 34 ^{o}, 55 ^{o} and 65^o related to SiO_2 pattern. The patterns are found to be in good agreement with the standard peak positions of $SnZnO_3$. These peaks reveal that all the investigated samples are nano crystalline powder of hexagonal wurtzite structure. The crystallite size of $Si_{0.5}Sn_{0.5}ZnO_3$ powder was 18-27nm which calculated using Scherrer's formula and the data is given in Table 3.

Figure 1 (b) depicted the X-ray diffraction of the $SrTiO_3$ ceramic target prepared using the conventional powder processing unit. The pattern of the target investigated in the range of 2θ (20° ~90°). The pattern has been indexed with $SrTiO_3$, the peak planes of cubic symmetry of $SrTiO_3$ are 311, 100, 111, 200, 211, 220 appeared at its position, which well matched with the Card no. 35-0734.[35)]

The XRD pattern of as-synthesized ceramic thin films of $Si_{0.5}Sn_{0.5}ZnO_3$ deposited on both the substrates of MgO and STO/MgO by PLD depicted in Fig. 2 (a, b). The crystal structure is a typical face centered cubic (FCC) of the synthesized films which is the perovskite structure (JCPDS no.: 11-0274). The pattern is polycrystalline and most of the peaks indexed with $ZnSnO_3$.

No diffraction peaks due to impurities or other crystalline by products such as ZnO or SnO_2 were detected, indicating that pure $ZnSnO_3$ crystallites could be obtained under present synthesis conditions.[34)] There are included five peaks corresponding to the 002, 111, 100, 200, and 222 reflections of MgO-substrate, demonstrating that the film was highly oriented.

Fig. 2 (b) shows the pattern of the $Si_{0.5}Sn_{0.5}ZnO_3$ films on the STO-substrate. As it is clear from the pattern the polycrystalline film is oriented and all peaks indexed with the standard $ZnSnO_3$ with the perovskite structure (JCPDS no.: 11-0274). Only two peaks appeared at 2θ equals 34° and 70° related to 110 and 220 plans of $SrTiO_3$. The XRD data confirmed the adjustment of the films on STO substrate due to the mismatch between $Si_{0.5}Sn_{0.5}ZnO_3$ film and MgO-substrate. For growing the perovskite films, MgO wafer can be chosen as a substrate material for various purposes. The lattice parameter of MgO (a_o =4.213 Å) is relatively fitted to the lattice parameters of $Si_{0.5}Sn_{0.5}ZnO_3$ (a=3.994 Å, c=4.038Å). In addition, the refractive index of MgO is smaller than $Si_{0.5}Sn_{0.5}ZnO_3$ enabling wave guiding in thin $Si_{0.5}Sn_{0.5}ZnO_3$ films. MgO prevents a linear electro-optic effect.[12] Because MgO has smaller refractive index than $Si_{0.5}Sn_{0.5}ZnO_3$ along with the small optical loss, a $Si_{0.5}Sn_{0.5}ZnO_3$/MgO structure is advantageous for application of waveguide applications. The purpose of STO as a buffer layer decreases difficulties correlated to inter dispersion and oxidation which are common for these semiconductor substrates. Therefore, STO looks to be a proper material for purpose in combined optics in that it would be an integral part of a waveguide device as well as allow for the growth of high quality $Si_{0.5}Sn_{0.5}ZnO_3$ thin films on semiconductor substrates. Optimum deposition conditions have been done for getting well ferroelectric state for this $Si_{0.5}Sn_{0.5}ZnO_3$ thin film. Only MgO can be good substrate for $Si_{0.5}Sn_{0.5}ZnO_3$ ferroelectric thin film deposition. In addition to this study confirmed that STO-substrate improve the ferroelectricity of the $Si_{0.5}Sn_{0.5}ZnO_3$ ceramic thin films.

Figure 3 presented the FE-SEM image for the $Si_{0.5}Sn_{0.5}ZnO_3$ films grown on the STO and MgO substrates. The average particles size of the films on MgO and STO/MgO are around 50 nm and 90 nm, respectively.

The thickness of the films is 150 and 220nm, whilst the annealing temperature is 650^{o}C during time interval are 2h and 4h for the films on MgO and STO/MgO substrates, respectively. The grain growth process exhibited for the films grown on the substrate of STO due to the longer time of annealing (4h).

From the XRD analysis, it is shown that the $SrTiO_3$ buffer layer has a noticeable influence on the structure of the $Si_{0.5}Sn_{0.5}ZnO_3$ films. So, it is important to explain the main reasons for selecting STO material as a buffer layer in the current work. For numerous reasons, the STO was chosen as a buffer layer between the MgO substrate and $Si_{0.5}Sn_{0.5}ZnO_3$ film. STO is a linear dielectric material with excellent insulating properties, and the components of the two systems are similar, reducing dislocations and defects at the interface.

Figure 4 (a-d) depicts the polarization and electric field (ferroelectric hysteresis loops) of different thicknesses of $Si_{0.5}Sn_{0.5}ZnO_3$ growth on substrates of MgO and $SrTiO_3$ at ambient temperature. Figure 4 (a) shows a ferroelectric hysteresis loop of Si-doped thin film at 150 nm thickness in MgO substrate which has a lossy capacitor response. Whereas Figure 4 (c) represents the E-P loop of 150 nm thickness of the same film growth on STO substrate in the same preparation condition which has a non-linear ferroelectric response. This indicates that the liner dielectric layer (STO) buffer layer improves the ferroelectric behavior of $Si_{0.5}Sn_{0.5}ZnO_3$ thin films compared to the MgO substrate which is consistent with structure results. To confirm this response, the different film thicknesses of Si-doped $SnZnO_3$ growth films on both substrates are examined. In figure 5, just two thicknesses for each prepared sample are presented whereas the rest of the results are presented in the supplementally sheet (Figures 6, 7). By comparing Figure (4-b) and figure (4-d), which represent the thin film at 250 nm thickness deposited on MgO and STO substrate respectively, Both films as same response as for 150 nm thickness. This confirmed that the shape and area of the P–E hysteresis loop of Si-doped $SnZnO_3$ changed by adding an STO buffer layer. The ferroelectric parameters of prepared samples depicted from P-E hysteresis such as the maximum polarization (P_m), remanent polarization (Pr), coercive fields (E_{co}), and energy losses (A) are gathered in the Table (1).

Figure 5 represents the variation of the ferroelectric parameters with the thin film thickness in both substrates. It is obvious to notice that all ferroelectric parameters of thin films on STO substrate are greater than those of thin film on MgO substrate for all thicknesses by a different order of magnitude. This indicates that the improvement of ferroelectric properties of the prepared thin film on the substate has a linear STO dielectric layer. Also, it is observed that for Figure 6-a that remanent polarizations of STO samples decrease with film thickness till 200 nm after that it increased. It is known that Pr could be affected by the changing of ferroelectric domains, crystallinity and grain sizes. Moreover, due to preparation conditions of the sample's preparations being the same. So, it could be a change in the morphology of film as the thickness is changed. Also, the same behavior was observed for the change of E_{co} with the change of the film thicknesses on the STO substrate.

Figure 8 shows the atomic force microscope (AFM) images of different thicknesses of thin film on STO substrate. The roughness of AFM images is summarized in Table 2. It is found that the film roughness is decreased as the film thickness to 200 nm after that the roughness is increased. This indicated that the film morphology could affect the ferroelectric properties such as P_r, and E_{co}.

Likewise, the STO-layer between MgO-substrate and $Si_{0.5}Sn_{0.5}ZnO_3$ ceramic films is play an important rule for the modification of the lattice parameter mismatch between $Si_{0.5}Sn_{0.5}ZnO_3$ films and MgO layer.

Figure 9 illustrates a relation between the current density and applied electric field (J-E) of the $Pt/Si_{0.5}Sn_{0.5}ZnO_3/MgO/TiO_2/Pt$ and $Pt/Si_{0.5}Sn_{0.5}ZnO_3/SrTiO_3/MgO/TiO_2/Pt$ films. The current density of the $Si_{0.5}Sn_{0.5}ZnO_3$ film grown on the STO substrate decreased compared to that of the $Si_{0.5}Sn_{0.5}ZnO_3$ grown on the MgO substrate. The values for $Si_{0.5}Sn_{0.5}ZnO_3$/STO and $Si_{0.5}Sn_{0.5}ZnO_3$/MgO thin films at higher electric fields of 40 and 8 kV/cm were 6×10^{-8} and 9×10^{-6} A/cm^2, respectively. The experimental data confirmed the effect of dielectric nature of the STO buffer layer on the interface of the film on the STO, that decreased the leakage current in the films. In addition to the semiconductor nature of the MgO layer increased the current density of the film influenced the electric properties of the grown films. This indicates that the film's condition was enhanced and that layer of STO property between the $Si_{0.5}Sn_{0.5}ZnO_3$ and STO was better than that between $Si_{0.5}Sn_{0.5}ZnO_3$ and MgO substrates. One note here is the A-site doping of ferroelectric perovskite enhanced ferroelectricity and leakage current. In addition, the leakage current density decreased by around 8% of its value of the films with MgO. Our data make us to believe the improvement of remanent polarization of the polycrystalline $Si_{0.5}Sn_{0.5}ZnO_3$ films because of the good choice of the interface between the films and the substrate ($SrTiO_3$). Our data results of polarization of $Si_{0.5}Sn_{0.5}ZnO_3$ thin films are considered as new data for first time, the objects of this paper are achieved; firstly, doping Si-content and secondly STO layer as buffer layer for substrate.

The electrical parameters of $Si_{0.5}Sn_{0.5}ZnO_3/SrTiO_3$ and $Si_{0.5}Sn_{0.5}ZnO_3$/MgO films was measured using Hall experiment. The experimental data Tabulated in Table (3). The resistivity of the film's values is 3.22×10^3 and 7.35×10^7 $\Omega^{-1}.m^{-1}$ on the MgO and STO substrates, respectively. Indicating the electrical parameters of the films depends on the substrates type, since the semiconductor and insulating states of MgO and STO substrates. Further, the mobility of carriers in the films is 4.31×10^3 and 63.1 m/(V·s) for MgO and STO substrates, respectively.

Both the experimental data from Hall measurement and current density confirming the improvement of the ferroelectric properties of the $Si_{0.5}Sn_{0.5}ZnO_3$ films using the $SrTiO_3$ layer between the film and MgO-substrate.

Conclusion

To conclude, $Si_{0.5}Sn_{0.5}ZnO_3$ ceramic films were grown on $SrTiO_3$ and MgO substrates by pulsed laser deposition technique. The structure was investigated using XRD, FE-SEM and AFM confirmed the polycrystalline orientation of the films and smaller size nanoparticles of the films on MgO and large particle size of the films on the STO substrate. The STO buffer layer improve the ferroelectric state of the $Si_{0.5}Sn_{0.5}ZnO_3$ films. Further the films grown on STO substrate has smaller current density than the film on MgO substrates. The resistivity and mobility of carriers of the $Si_{0.5}Sn_{0.5}ZnO_3$ film's values are 3.22×10^3, $7.35\times10^7\ \Omega^{-1}.m^{-1}$ and 4.31×10^3, 63.1 m/(V·s) on MgO and STO substrates, respectively. The measured electric parameters confirmed the semiconductor and insulating states of the films on MgO and STO substrates. The experimental results confirmed both the Si-element and STO buffer layer adjusted the ferroelectricity in $SnZnO_3$ ceramic films.

Declarations

Acknowledgements

Ahmed I. Ali acknowledge the support and measuring some of the data in University of Ulsan, Ulsan, South Korea.

Compliance with Ethical Standards

Conflict of interest. The authors declare that they have no conflict of interest, and all co-authors have approved the contents of this manuscript and submission.

Competing Interests

The authors declare that they have no known competing financial interests or personal relationships that could have appeared to influence the work reported in this work.

Data availability and Materials

The authors confirm that the data supporting the findings of this study are available within the article. However, the original collected Data are available by contacting the corresponding author. Also, the IFEFFIT code used during the study are available online in accordance with funder data retention policies (the authors provide full citations that include URLs or DOIs.)

Funding

The author, Ahmed I. Ali acknowledges facility of both University of Ulsan, Ulsan, South Korea and NTRC at British University in Egypt for characterization and measurements. However, there is no funding for publication fees.

Author contributions

All authors have contributed, discussed the results, and approved the final manuscript.

References

1. Tae Yun Kim, Sung Kyun Kim and Sang-Woo Kim, “Application of ferroelectric materials for improving output power of energy harvesters”, Nano Convergence (2018) **5**, 30. https://doi.org/10.1186/s40580-018-0163-0
2. Ahmed I Ali, Mansour M Hassan, G Goda Mohammed, Hossam Youssef Abdel El-hamid, Hilmy Awad, “Preparation, Structural and Dielectric Properties of Nanocomposite Al_2O_3/$BaTiO_3$ for Multilayer Ceramic Capacitors Applications”, Journal of Materials Research and Technology, Volume 18, May–June (2022), Pages 2083-2092. https://doi.org/10.1016/j.jmrt.2022.03.041.
3. A. Abdel Moez, Y. S. Kim & Ahmed I. Ali, “Investigation of structure, optical, nonlinear optical, dialectical properties and electronic results of $La_{0.01}Ba_{0.99}TiO_3$, $Sm_{0.5}Sr_{0.5}CoO_3$ and $Sm_{0.5}Sr_{0.5}CoO_3$ /$La_{0.01}Ba_{0.99}TiO_3$thin films grown on quartz substrates using pulsed laser deposition (PLD) technique”, Journal of Optics,1-11 (2021). (https://link.springer.com/article/10.1007%2Fs12596-021-00703-0).
4. Ahmed I. Ali & A. Hassen, “Synthesis, characterization, ferroelectric, and piezoelectric properties of (1 − x)$BaTiO_3$−x($BaNi_{0.5}Nb_{0.5}O_3$) perovskite ceramics”, Journal of Materials Science: Materials in Electronics volume 32, pages10769–10777 (2021). https://link.springer.com/article/10.1007/s10854-021-05734-8
5. Ahmed I. Ali, H A El Meleegi and A Abdel Moez “Investigation of structural, optical dielectrical and optical conductivity properties of $BaTiO_3$, $Al_{0.01}Ba_{0.99}TiO_3$ and $La_{0.01}Ba_{0.99}TiO_3$ thin films prepared by pulsed laser deposition” , Physica Scripta, Volume 94, Number 12 (2020) p125810.https://doi.org/10.1088/1402-4896/ab1f25
6. Ahmed I Ali, S. El-Sayed and A Hassen,“Change the ferroelectric properties of $Al_{0.\ 01}Ba_{0.99}TiO_3$ ceramics by $Al_{0.01}$Sr0. $_{99}TiO_3$ doping”, Results in Physics 14, 102368, (2019).
7. Ahmed I Ali, A Hassen, Nguyen Cao Khang, YS Kim, “Ferroelectric, and piezoelectric properties of $BaTi_{1-x}Al_xO_3$, $0 \leq x \leq 0.015$”, AIP Advances (5), 9, 097125 (2015).
8. Ahmed I. Ali, Kim Il-Won, and Y. S. Kim "The influence of $SrTiO_3$ buffer layer on ferroelectric properties of Al-doped $BaTiO_3$ thin films**",** (**Journal of Electroceramics; V32, N (1) (2014).**
9. Ahmed I. Ali, Amir Ullah, Kibog Park, Rock Huh, Y. S. Kim “Ferroelectric Enhancement of La-Doped $BaTiO_3$ Thin Films Using $SrTiO_3$ Buffer Layer, Thin Solid Films 551 (2014) 127–130.
10. Ahmed I. Ali, C.W. Ahn, Y. S. Kim, “Enhancement of Piezoelectric and Ferroelectric Properties of $BaTiO_3$ Ceramics by Aluminum Doping”, Ceramics International, Volume 39, Issue 6, August 2013, Pages 6623-6629.
11. Ahmed I. Ali, A. Abed Al Moez, and Y. S. Kim, "Hall mobility, resistivity and dielectric properties of reduced $La_{0.01}Ba_{0.99}TiO_3$", Journal of Korean Physical Society, 62 (7), (April 2013)1024-1030).

12. Ahmed I. Ali, Saleh H. Kaytbay, "Electrical Transport Properties of La-$BaTiO_3$" Materials Sciences and Application 2, 716-720 (2011).
13. J. Y. Son, Young-Han Shin, Han-Bo-Ram Lee and H. Kim, J. H. Cho, and Ahmed I. Ali, "Surface Charge on Ferroelectric Thin Film by High Electric Field Induced at Scanning Probe Microscope Tip", Journal of the Korean Physical Society 51, S125-S128 (2007).
14. B. H. HOERMAN, G. M. F., L. D. KAUFMANN and B. W. WESSELS, “Dielectric properties of epitaxial thin films.”, Appl. Phys. Lett. 1998, 73, 2248.
15. S . KIM, T. F., T. MANABE, I . YAMAGUCHI, T. KUMAGAI and S . MIZUTA,” Dense and smooth epitaxial BaTiO3 thin films by the dipping-pyrolysis process” J. Mater. Res. 1999, 14, 592.
16. H. BASANTAKUMAR SHARMA, H. N. K. S. a. A. M. “Fatigue in sol-gel derived barium titanate films”, J. Appl. Phys. 1999, 85, 341.
17. K.Y. Lee, D. Kim, J.H. Lee, T.Y. Kim, M.K. Gupta, S.-W. Kim, “Unidirectional High-Power Generation via Stress-Induced Dipole Alignment from $ZnSnO_3$ Nanocubes/Polymer Hybrid Piezoelectric Nanogenerator”, Adv. Funct. Mater. 24, 37 (2014).
18. A.G. Luchaninov, A.V. Shil’nikov, L.A. Shuvalov, V.A. Malyshev, “The effect of mechanical stress on the properties of electrically depolarized piezoelectric ceramics”, Ferroelectrics 145, 235 (2011).
19. T. Kumazawa, Y. Kumagai, H. Miura, M. Kitano, K. Kushida, “Effect of external stress on polarization in ferroelectric thin films”, Appl. Phys. Lett. 72, 608 (1998).
20. A. Gruverman, B.J. Rodriguez, A.I. Kingon, R.J. Nemanich, A.K. Tagantsev, J.S. Cross, M. Tsukada, “Mechanical stress effect on imprint behavior of integrated ferroelectric capacitors”, Appl. Phys. Lett. 83, 728 (2003).
21. D. Yang, L.Q. Zhang, H.L. Liu, Y.C. Dong, Y.C. Yu, M. Tian, “Lead magnesium niobate-filled silicone dielectric elastomer with large actuated strain”, J. Appl. Polym. Sci. 125, 2196 (2012).
22. S. M. Bobade, D. D. G., A. R. Kulkarni, and P. Gopalan, “Dielectric properties of A- and B-site-doped BaTiO3(l):LaBaTiO3(l):La- and Al-doped solid solutions”, J. Appl. Phys. 2005, 97, 074105.
23. O.D. Jayakumar, S. N. A., K.G. Girija, A.K. Tyagi, C. Sudakar, G. Lawes, R. Naik, J. Nisar, X. Peng, R. Ahuja, “Theoretical and experimental evidence of enhanced ferromagnetism in Ba and Mn substituted $BiFeO_3$”, Appl. Phys. Lett. 2010, 96, 032903.
24. Z.X. Cheng, X. L. W., S.X. Dou, H. Kimura, K. Ozawa, “Enhancement of ferroelectricity and ferromagnetism in rare earth element doped BiFeO3”, J. Appl. Phys. 2008, 104, 116109.
25. J. Xu, G. W., H. Wang, D. Ding, Y. He, “Synthesis and weak ferromagnetism of Dy-doped $BiFeO_3$ powders”, Mater. Lett. 2009, 63, 855.
26. B. Xu, K. B. Y., J. Lin, Y.D. Xia, X.G. Wan, J. Yin, X.J. Bai, J. Du, Z.G. Liu, “Room-temperature ferromagnetism and ferroelectricity in Fe-doped $BaTiO_3$”, Phys. Rev. B 2009, 79, 134109.
27. Y.-H. Lin, J. Y., S. Zhang, Y. Zhang, J. Liu, Y. Wang, C.-W. Nan, “Multiferroic behavior observed in highly orientated Mn-doped BaTiO3BaTiO3 thin films”, Appl. Phys. Lett. 2009, 95, 033105.

28. J.M.D. Coey, M. V., C.B. Fitzgerald, “Donor impurity band exchange in dilute ferromagnetic oxides”, Nat. Mater. 2005, 4, 173.
29. D.B. Buchholz, R. P. H. C., J.H. Song, J.B. Ketterson, “Room-temperature ferromagnetism in Cu-doped ZnO thin films”, Appl. Phys. Lett. 2005, 87, 082504.
30. Ju, H. L.; Eylem, C.; Peng, J. L.; Eichhorn, B. W.; Greene, R. L.” Metal-insulator transitions and weak ferromagnetism in the electron-correlated system $Nd_{1-x}Ca_xTiO_3$ ($0 \le x \le 1$)”, Physical Review B 1994, 49, 13335-13341.
31. Yao, J.; Xiong, C.; Dong, L.; Chen, C.; Lei, Y.; Chen, L.; Li, R.; Zhu, Q.; Liu, X. “Enhancement of dielectric constant and piezoelectric coefficient of ceramic–polymer composites by interface chelation” Journal of Materials Chemistry 2009, 19, 2817-2821.
32. L. A. WILLS, B. W. W., D. S. RICHESON and T. J . MARKS “Second-harmonic generation of poled $BaTiO_3$ thin films”Appl. Phys. Lett. 1992, 60, 41.
33. T. HAYASHI, N. O. a. H. M. “The effect of interface oxygen content on magnetoelectric effect of epitaxial $La_{0.7}Sr_{0.3}MnO_3/BaTiO_3$ bilayer,”Jpn. J. Appl. Phys. 1994, 33 (9B), 5277.
34. Jiaoling Zheng, Huanhuan Hou, Hao Fu, Liping Gao and Hongjie Liu, “Size-controlled synthesis of porous $ZnSnO_3$ nano cubes for improving formaldehyde gas sensitivity”, RSC Advances, 2021,11, 20268.
35. Huang, S.-T.; Lee, W.W.; Chang, J.-L.; Huang, W.-S.; Chou, S.-Y.; Chen, C.-C. Hydrothermal synthesis of $SrTiO_3$ nanocubes: Characterization, photocatalytic activities, and degradation pathway. J. Taiwan Inst. Chem. Eng. 2014, 45, 1927–1936.

Tables

Tables 1 to 3 are available in the Supplementary Files section

Figures

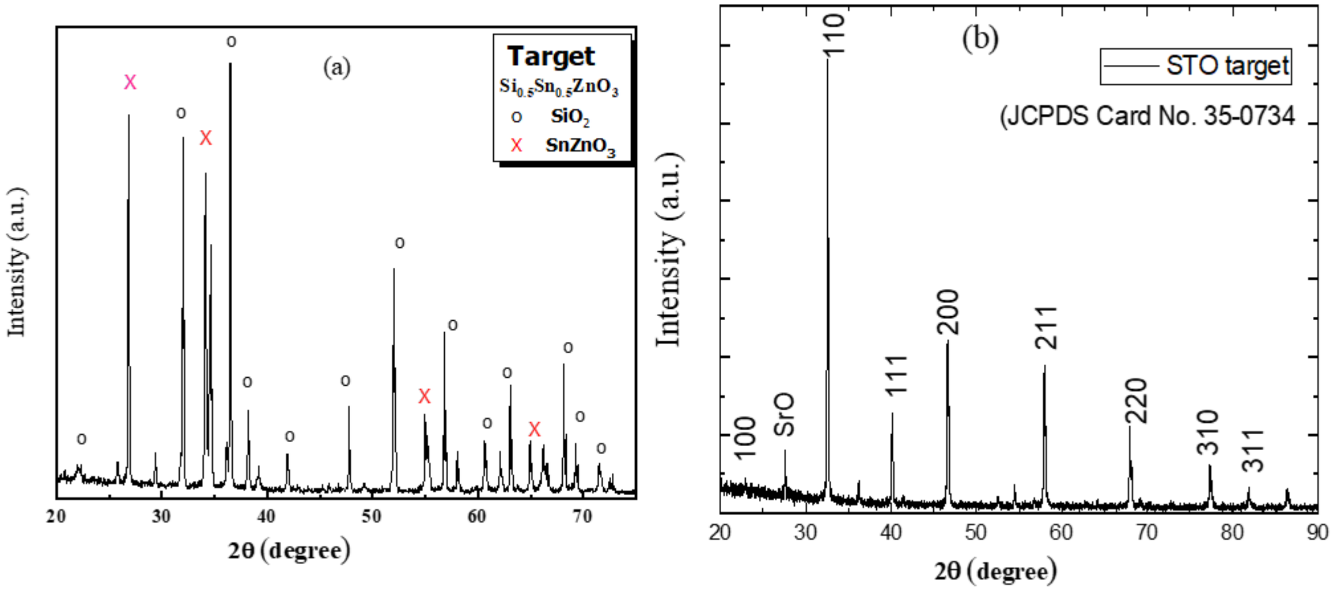

Figure 1

The XRD pattern of both targets of (a) $Si_{0.5}Sn_{0.5}ZnO_3$ and (b) $SrTiO_3$.

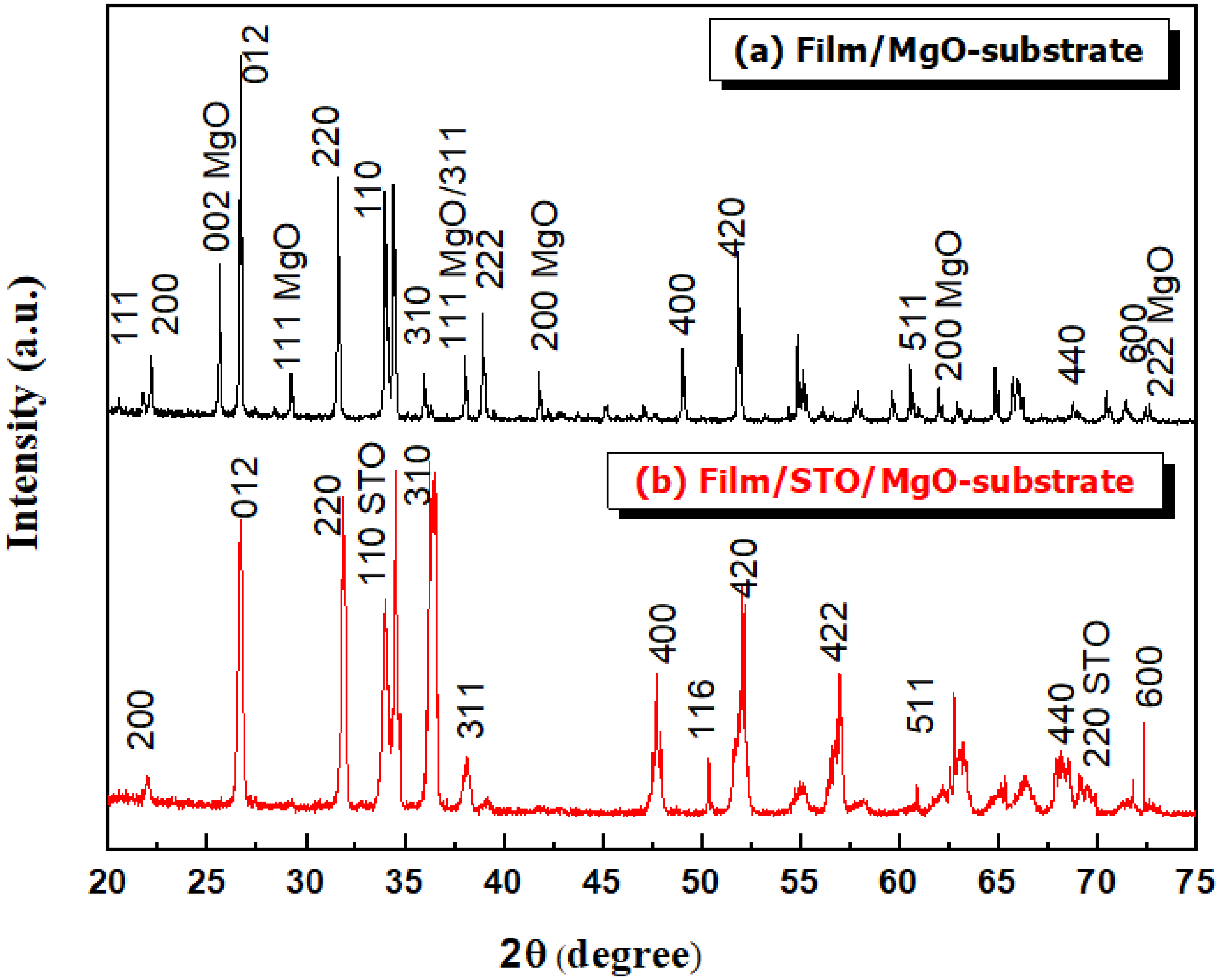

Figure 2

The X-Ray diffraction patterns of $Si_{0.5}Sn_{0.5}ZnO_3$ thin films grown on (a) $SrTiO_3$ and (b) MgO-substrates.

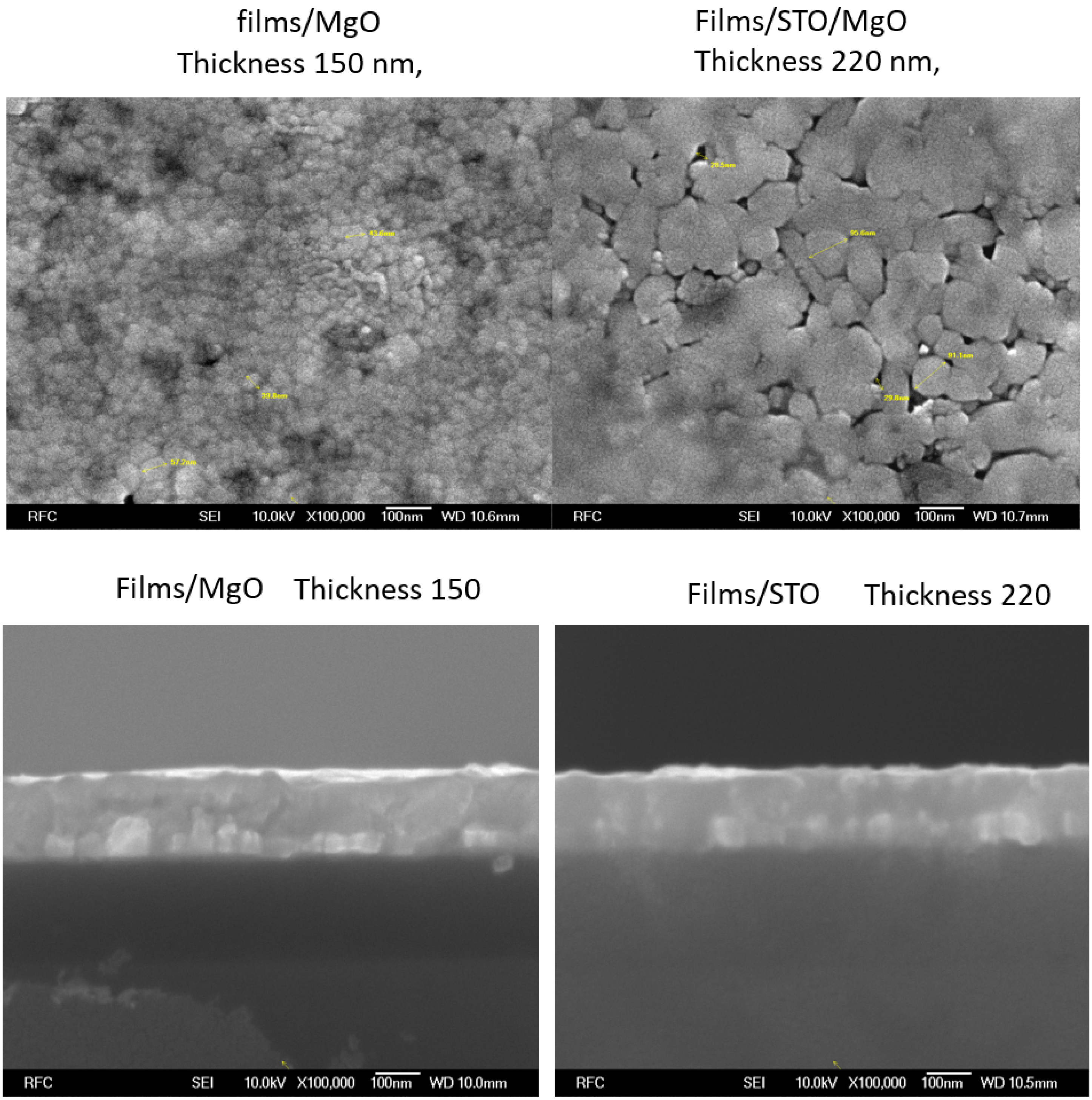

Figure 3

The FE-SEM image of $Si_{0.5}Sn_{0.5}ZnO_3$ thin films grown on (a) $SrTiO_3$/MgO and (b) MgO substrates. (c, d) the FE-SEM image of cross-sectional (thickness) of $Si_{0.5}Sn_{0.5}ZnO_3$ thin films grown on (a) $SrTiO_3$ and (b) MgO substrates by pulsed laser deposition.

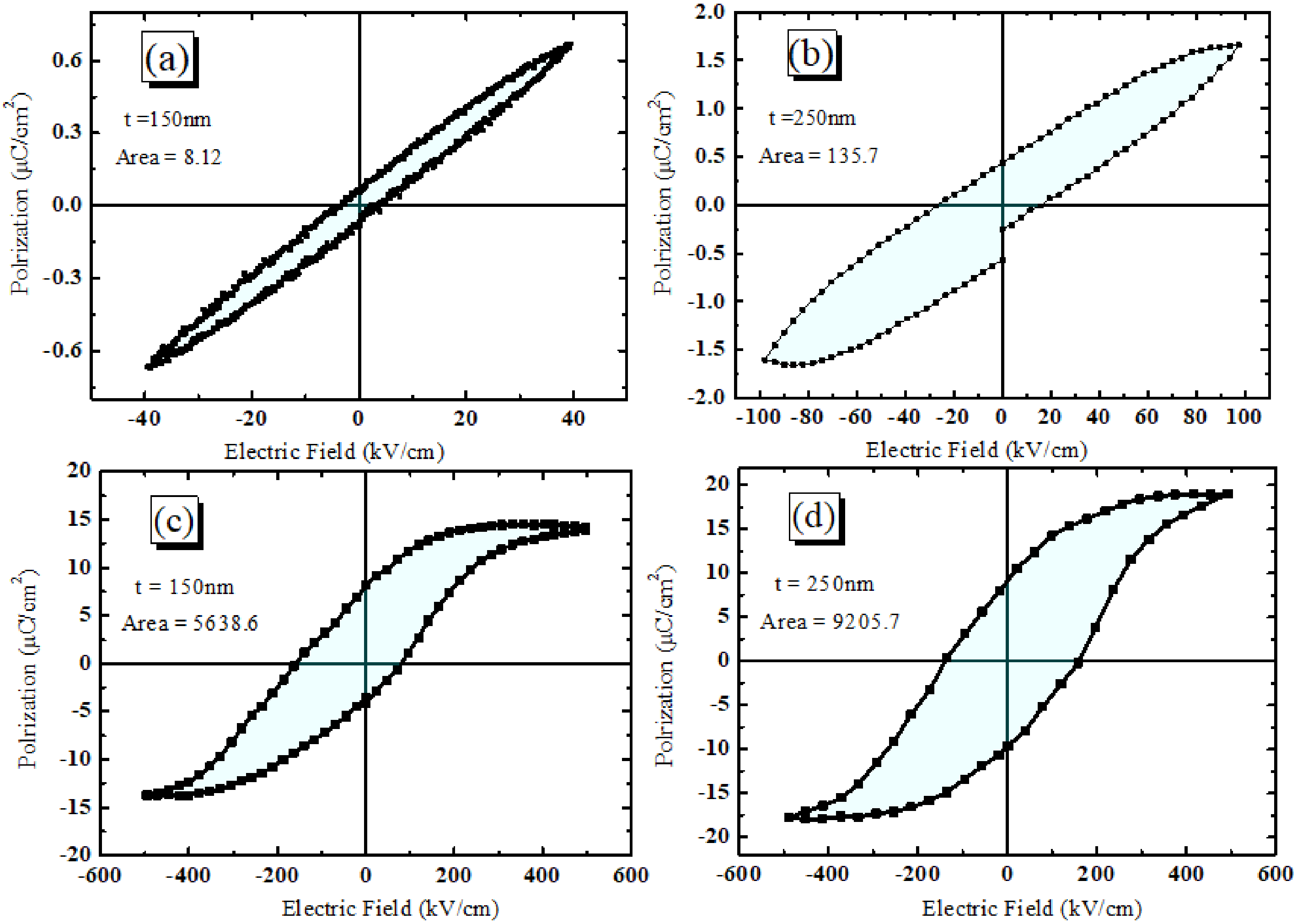

Figure 4

The Ferroelectric hysteresis loops of different thickness $Si_{0.5}Sn_{0.5}ZnO_3$ thin films grown on (a), (b) $MgO/TiO_2/SiO_2/Si$ substrate 150 nm and 250nm respectively, (c), (d) $SrTiO_3/MgO/TiO_2/SiO_2/Si$ substrate 150 nm and 250nm, respectively.

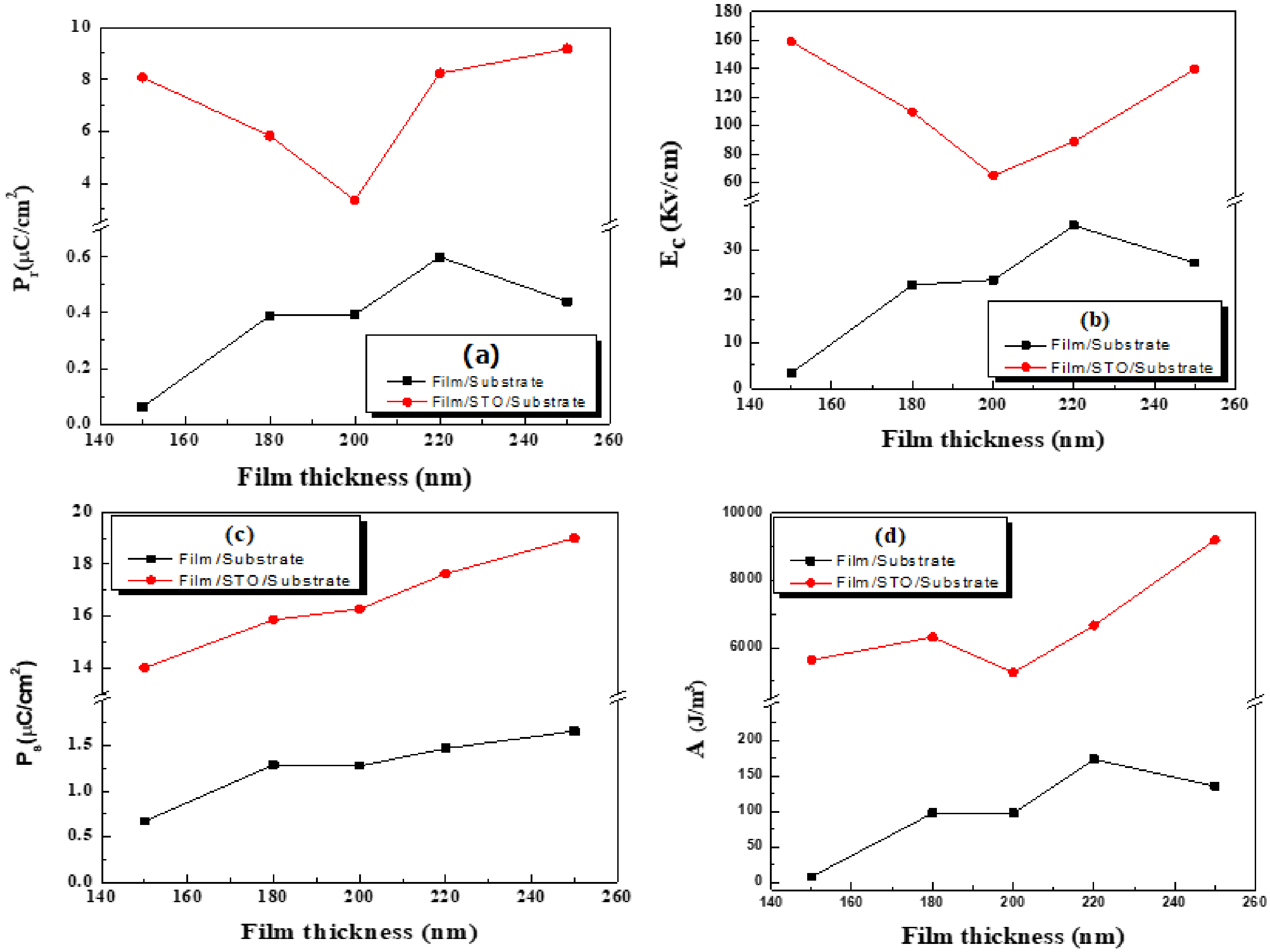

Figure 5

The Ferroelectric parameters of Si0.5Sn0.5ZnO3 thin films grown on SrTiO3/MgO/Pt/TiO2/SiO2/Si substrates by pulsed laser deposition.

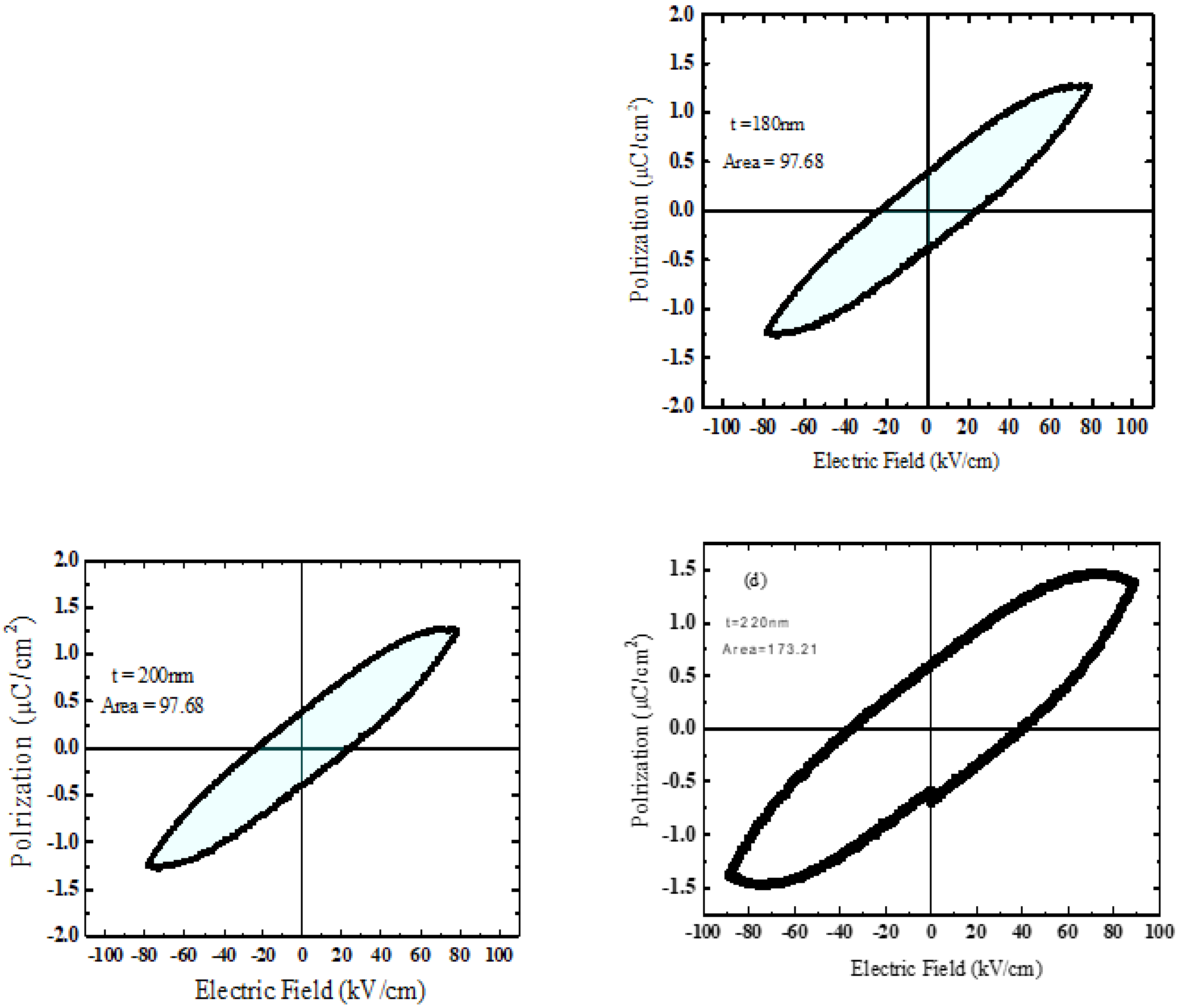

Figure 6

The Ferroelectric hysteresis loops of $Si_{0.5}Sn_{0.5}ZnO_3$ thin films grown on MgO- substrates at different film thicknesses (180, 200 and 220 nm) by pulsed laser deposition.

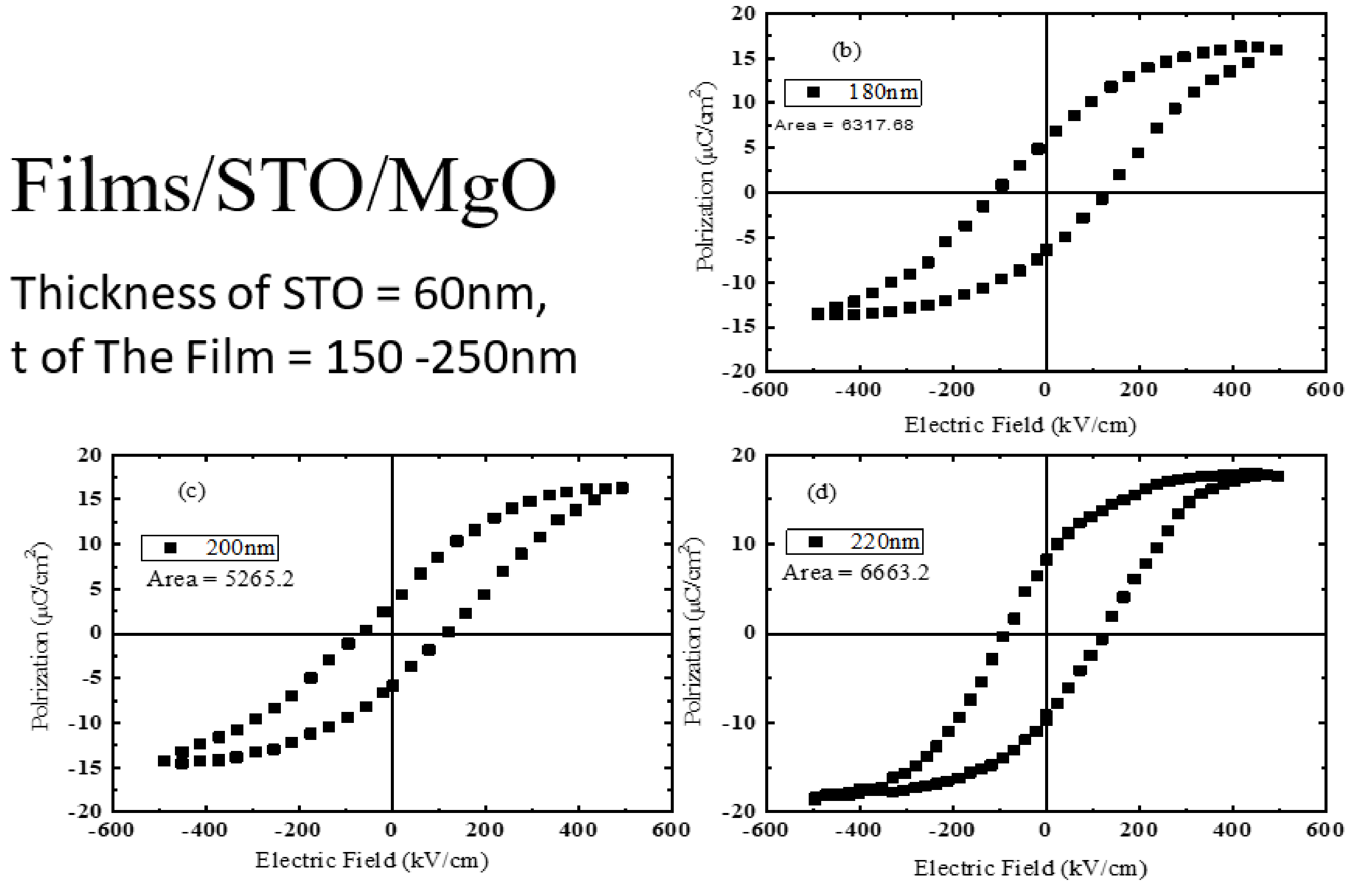

Figure 7

The Ferroelectric hysteresis loops of $Si_{0.5}Sn_{0.5}ZnO_3$ thin films grown on $SrTiO_3$/MgO- substrates at different film thicknesses (180, 200 and 220 nm) by pulsed laser deposition.

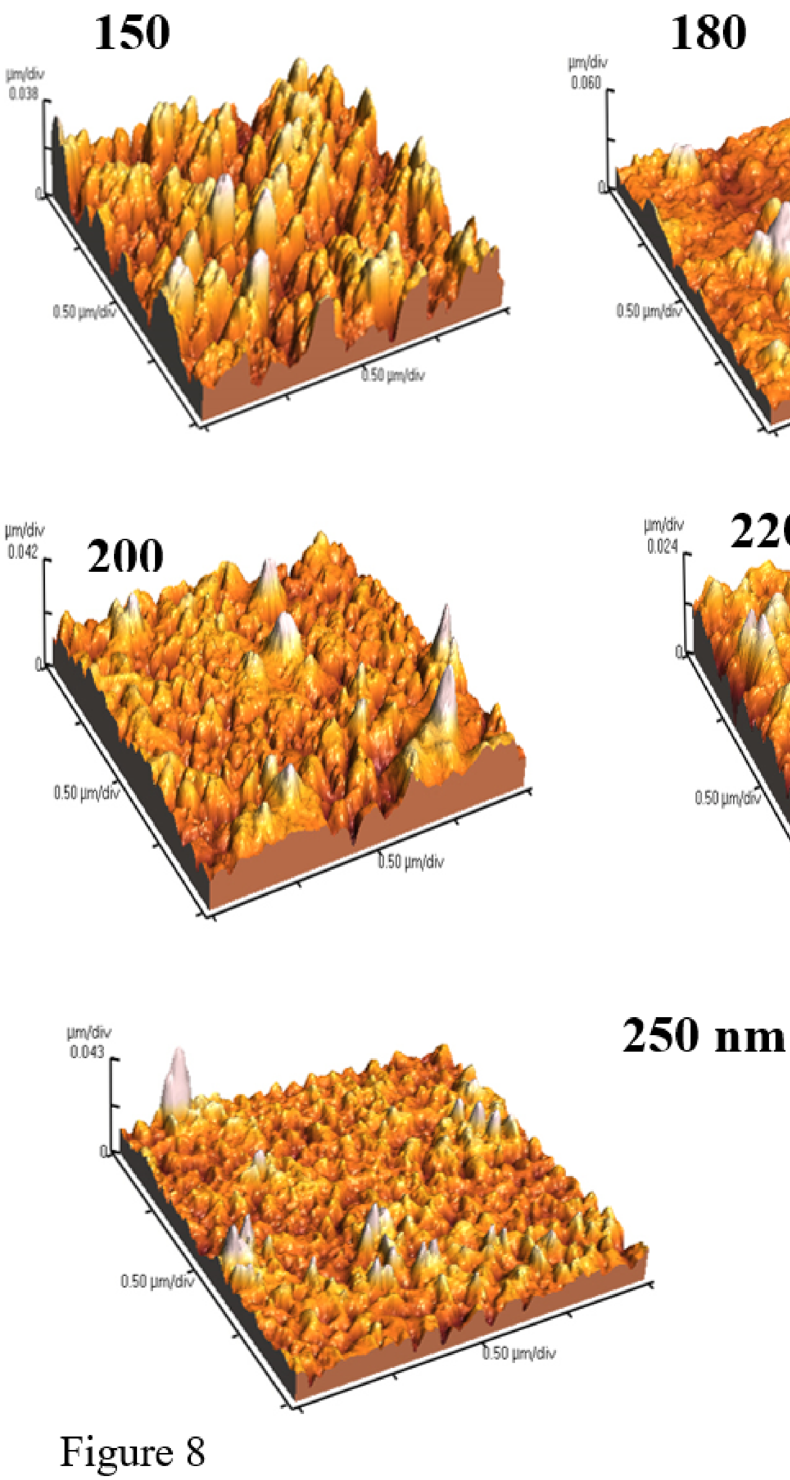

Figure 8

Atomic Force Microscopy of the $Si_{0.5}Sn_{0.5}ZnO_3$ thin films deposited on $SrTiO_3$/MgO- substrates at different thicknesses (180, 200, 220 and 250 nm) by pulsed laser deposition.

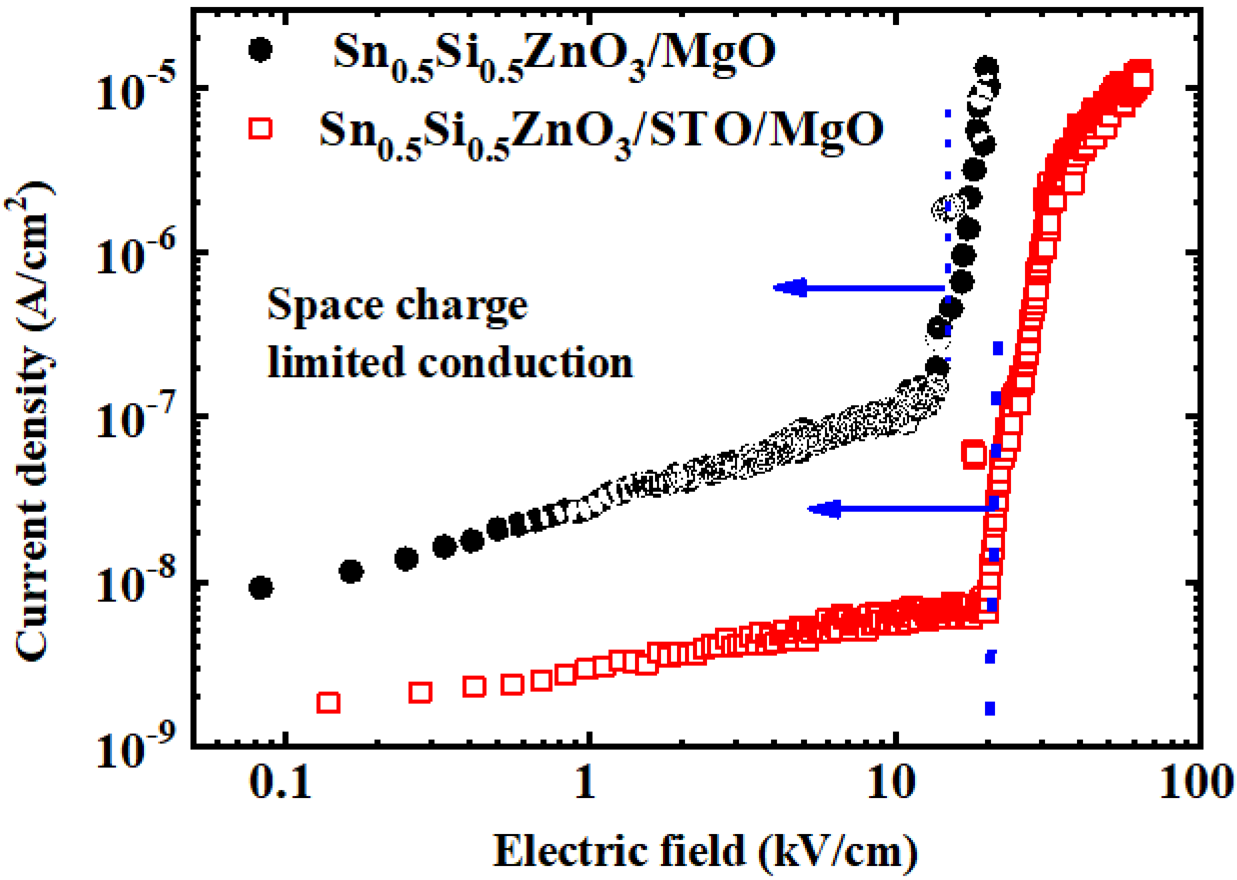

Figure 9

The leakage current density as a function of applied field curves of $Si_{0.5}Sn_{0.5}ZnO_3$ thin films grown on MgO and $SrTiO_3$ substrates by pulsed laser deposition.

Supplementary Files

This is a list of supplementary files associated with this preprint. Click to download.

- ListofTable.pptx